

# Effect of a Circular Cylinder as a Passive Controller on the Savonius Wind Turbine

Waleed A. Alaksar<sup>a</sup> and Mohamed H. Mohamed<sup>a,b</sup>

<sup>a</sup> Mechanical Engineering Dept, College of Engineering and Islamic Architecture, Umm Al-Qura University, P.O. 5555, Makkah, Saudi Arabia.

<sup>b</sup> Mechanical Power Engineering Department, Faculty of Engineering, Helwan University, Mattaria, Egypt.

## Abstract

Wind energy is becoming increasingly desirable in modern and family settings, and it is increasingly being used to replace traditional oil-produced energy. This can also help to reduce natural contamination. For low and high-power applications, various types of vertical axis turbines have been used. Because of its simplicity and advantages over horizontal hub wind turbines, vertical axis wind turbines have recently received more attention. Because of its simplicity, one of the most well-known varieties of a vertical pivot wind turbine is the Savonius, especially in places with low wind speeds. Installing a deflector on the Savonius turbine is a low-cost solution to boost its power performance. A circular cylinder system has been proposed in this paper as a passive control. In this work seven cases of controlling the circular cylinder location and diameter where the cylinder is installed on the upstream side of the returned blade cause the formation of a wake region between the cylinder and the returned blade; As a result, the change in pressure between the front and back sides of the returned blade

diminishes, lowering the pressure drag of the returned blade. As a result, the drag force of the returned blade decreases, resulting in a positive torque in the rotor and improving the performance of the Savonius turbine. The influence of the cylinder deflector on the Savonius turbine has been numerically studied by 2D CFD simulations using Inventor software to draw a 2D model of the turbine. The analyses were carried out utilizing the ANSYS Fluent and the Shear Stress Transport  $k-\omega$  turbulence model. The results proved that the inclusion of the circular cylinder as a passive control of the returned rotor blade can boost the Savonius turbine's efficiency. For numerical results, in case (RC2) the output power increases by installing the cylinder with (0.107m) diameter located in front of the returning blade where the increase in the maximum power coefficient reaches 46.6% at tip speed ratio equal to 1.

**Keywords:** Passive control; CFD; Power coefficient; Numerical; Circular cylinder; Tip speed ratio; Savonius turbine.

## Nomenclature

$A$	Rotor area (m <sup>2</sup> )	$t$	Blade thickness (mm)
$OL$	Overlap ratio	$R$	The radius of the rotor (m)
$d$	The cylinder diameter (m)	$h$	The height of the cylinder (m)
$A_s$	The swept area of blades (m <sup>2</sup> )	$RC$	Round cylinder
$\rho$	Air density (kg/m <sup>3</sup> )	$D_o$	Length of the outer domain (m)
$U$	Wind velocity (m/s)	$C_p$	Power coefficient
$C_{pmax}$	Maximum power coefficient	$Re$	Reynolds number
$\lambda$	Tip speed ration	$\omega$	Angular velocity (rpm)
$D$	Blade diameter (m)	$2D$	Two dimensional
$a$	Shaft diameter (m)	$M$	Moment
$S$	The horizontal distance (m)	$C_m$	Moment coefficient
$L$	Rotor overall diameter (m)		

## 1. INTRODUCTION AND BACKGROUND

The earth absorbs part of the radiation as the sun radiates. The warm soil heats the air above it. In what is called convection currents, hot air rises. Unbalanced heating of the surface of the ground produces winds. If, for instance, the rays of the sun come to earth and the oceans, the ground heats faster (hot air rises). Therefore, the cooler air would flood over the sea to fill the void left by the rising air. These are processes that generate high and low-pressure areas and cause winds. (Hadi Ali, 2013) Due to growing energy demand, traditional energy is becoming increasingly costly and scarce. Energy from renewables including wind, solar, tidal, and geothermal energies as well as biomass energy must be generated, so that the need for fossil energy can be decreased, fossil energy causes climate changes, such as global warming and acid rain, which has increased, primarily using fossil fuels in power generation and transport. Wind energy is a fossil energy substitute since it is clean, readily available, widely distributed, and generates lower gas emissions. (Barhoumi et al., 2020) Energy is related to the most social and economic issues impacting countries' sustainable growth. Saudi Arabia plans to use renewable energy sources to diversify its economic capital. Wind and solar power would make a major contribution to Saudi Arabia's future electricity. A specific strategy drawn up by the Higher Authority of the Ministry of Energy is aimed at generating more than 40 GW of renewable electricity by 2030. Research and growth, manufacture of machinery, and higher schooling for skills learning shall be part of the green energy supply chain. In both north and west of Saudi Arabia, it is seen that substantial wind energy occurs in Saudi Arabia. The Medina, Tabuk, Hail, Makkah, and Abha regions are the best places for wind turbine plants. (Alharbi & Csala, 2020) used the Brownian Motion (BM) and Monte Carlo Simulation (MCS) to do the future prediction of the wind and solar energy potential, three regions were selected in Saudi Arabia: the southern region, the northwestern region, and the middle region. The historical weather data had collected from eight weather stations for the three regions during the period (1950–2019), the results of this research show the north-western region has the best average wind speeds (from 5.8 to 8.5 m/s) and the southern region was the second promising region which showed satisfy performance for daily average wind speed (between 4.8 m/s and 8.57 m/s). (Said et al., 2004) The wind map of Saudi Arabia shows that the Kingdom is marked by two large windy regions along the Red Sea and the Arabian Gulf. In these two windy regions, the average annual wind speed is more than 9 knots (16,7 kmph) and ranges from 14 to 22 km/h and from 16 to 19 km/h over the Gulf of Arabia and the Red Sea coast. (Sakti & Yuwono, 2021) presented a numerical and experimental study aimed at improving the wind turbine's efficiency in Savonius. It is done by introducing a circular cylinder on the upstream side of the blade returned as passive control and a ratio of its diameter to the rotor diameter ( $d/D$ ) of 0.54. The cylinder placed at a distance ratio to the turbine rotor diameter ( $S/D$ ) is 1.4, at ( $Re$ ) Reynolds number = 140,000. Both results have shown that the circular cylinders would improve the Savonius turbine's performance, where a rise in the max power coefficient of approximately 10.2% and 8.8% was achieved for experimental and numerical work, respectively. (Shaheen et al., 2015) developed a multi-turbine group to build

efficient patterned savonius turbine farms, where they did numerical solutions for the savonius turbine in three stages (single turbine, a group of two turbines in oblique and parallel positions, and a triangular group of three savonius turbines facing the wind forwards and backward. The created three turbine bunch has an average power coefficient up to 34% higher than the single turbine. Numerical simulation for a cluster of savonius turbines as a building unit for efficient VAWT farms where two and three turbine configurations simulation showed enhanced performance and more efficiency compared to isolated turbines. Where the optimum gap distance for two parallel turbines is 0.2 times the rotor diameter. (Sobczak et al., 2020) A Savonius turbine concept with variable geometry of blades was presented. During the rotor revolution, blades constructed of an elastic material were continuously bent to enhance the positive torque of the advancing blade while decreasing the negative moment of the returning blade by using computational solid mechanics (CSM) simulations, and computational fluid dynamics (CFD) simulations. The aerodynamic performance improved as the deformation magnitude rose. The maximum of  $C_p$  was attained at the angle of  $105^\circ$  to be 0.30. However, the turbine's design is more complicated than the original. (Roy et al., 2018) used differential evolution to optimize the dimensions of a conventional bladed turbine-style which reduced the overall area SWT up to 9.8% Compared with previous experimental studies, According to the study, aspect ratio regulating parameters such as turbine elevation and radius of curvature are significant elements controlling the power and torque production from SWTs. (Mohamed H. Mohamed et al., 2021) introduced two directing plates on the savonius turbine, the first plate is an obstacle that safeguards the returning edge blade and the second plate is a deflector that allows the advancing blade to have better inflow conditions. The establishment of the front-facing directing plates upgrades the self-starting capacity for all shapes. by using a completely programmed optimization method (The streamlining depends on Evolutionary Algorithms) the ideal place of the redirecting plate was gotten taking in the thought the increasing of the power and torque coefficients there was a fantastic increment in the performance of the Savonius turbine has been reached 39.8%. (Bouzaher, 2022) proposed circularly deformable edges to work on the productivity of the Savonius vertical hub wind turbine. During turbine turn, the deformable blade changes shape. The advancing blade's elliptic extension enhances positive torque, while the returning blade's constriction reduced negative torque, greatly develops significantly turbine performance, this 2D study showed that the elliptic twisting along the x-axis further develops the turbine performance by over 90.6% during proper operating conditions, while the elliptic deformable along Y-axis worse performed than X-mode. (Alizadeh et al., 2020) applied an analysis study by using the SST Transition model on the impact of a circular obstruction on the Savonius hydrokinetic turbine. The circular obstruction intended to deflect the liquid stream from the returning blade's curved side to the advancing blade's sunken side. The torque was improved by 19% comparative with the base turbine. (Hassan Saeed et al., 2019) choose a 2D unsteady computational, Realizable of  $k-\epsilon$  was decided to be the turbulence model to achieve the validation, the investigation has been done on the impact of

blade shape modification to achieve the greatest value of power coefficients, four-rotor edge changes have been considered in this review: conventional, elliptical, utilizing Familiar Adjoint solver, and a unique blade design. The unique blades were predicted as a result of the Adjoint solver improvement, and the percentage of  $C_p$  increased to 23.9 percent. Furthermore, the effect of the blade's number was investigated by comparing two and three blades, with the result confirming that the three blades reduce  $C_p$  by 17.2%. (Submitted, 2017) optimized the aerodynamic shape for the savonius turbine which resulted in significant power and torque coefficients enhancement by two methods, 1) the blade shape of a Savonius wind turbine has been improved using only a standard genetic algorithm, giving rise to a power coefficient advancement of 33.4 percent when compared to traditional Savonius turbines with semi-circular blade forms; 2) The island model genetic algorithm was used to optimize the shape and position of a flow deflector in front of the returning blade of a conventional Savonius rotor, resulting in a 91.6% increase. (Kacprzak & Sobczak, 2015) researched the effect of overlap on the Classical Savonius wind turbine's performance for a wide variety of overlap ratios, unsteady 2D and 3D numerical simulations were performed to confirm the accuracy of the computations, The results indicate that all turbines work at their best when the tip speed ratio is between 0.7 and 0.9. A good truth is that when the overlap ratio increases, the max performance of a savonius turbine goes towards higher TSR. TSR = 0.7 produces the highest value of the power coefficient for an overlap ratio of 0, while TSR = 0.9 produces high performance with an overlap ratio of 0.30. (Talukdar et al., 2018) studied the Savonius hydrokinetic turbine (SHT) parametrically depending on the number of blades, edge shapes, and immersing level. Experiments have been conducted to compare the performance of two and three-bladed SHT with classic semicircular blades, and their max power coefficients have been determined to be 0.28 & 0.17, respectively. Although the elliptical turbine is supposed to have better performance than the semicircular turbine in the literature on SWT, the current SHT investigation opposes the reported SWT results. This issue appears to be worth researching, therefore the elliptical SHT requires further investigations and studies. (Sanusi et al., 2016) made changes to the rotor blades of traditional Savonius turbines in order to increase performance. In this study, the rotor blade modification is a blade combination that combines a circle-shaped conventional model with a concave elliptical model. The study involves an experimental model that incorporates a turbine prototype with 3 different blade versions with the same dimension in an open-jet-type flow tube. The experiment demonstrates that changing the rotor blade has an impact on the turbine's efficiency. At a tip speed ratio (TSR) of 0.79, the combined blade enhances the efficiency of ( $C_p$ ) by up to 11% over the traditional blade. (Ebrahimpour et al., 2019) investigated the effect of the overlap ratios in both horizontal and vertical directions on a conventional Savonius wind turbine with a constant diameter. Simulations were studied in this research utilizing computational fluid dynamics (CFD) and realizable K- $\epsilon$  turbulence model, as well as a the URANS equations. The findings revealed that near zero and positive horizontal overlap ratios yielded a higher overall efficiency than another states, the best model was a rotor with a horizontal

gap ratio of 0.15 and a vertical gap ratio of 0.1. (Mao & Tian, 2015) studied the influence of blade arc angle on the efficiency of a conventional Savonius rotor is explored using a transient CFD model in order to increase the turbine's power efficiency. K- $\epsilon$  turbulent system was used in the simulation, which was based on the Reynolds Averaged Navier–Stokes equations. Experimental results data were used to validate the numerical model. According to the findings, a turbine with a blade arc angle of  $160^\circ$  delivers the highest power coefficient, 0.28, which is 8.37 percent greater than a traditional Savonius wind turbine. (Alom et al., 2017) used the (FVM) solver ANSYS FLUENT with the SST k- $\omega$  turbulence model to run unsteady calculations and found that two-bladed turbines have a larger CP than three- and four-bladed turbines. A two-bladed turbine's maximum CP is roughly 1.5 times of a three-bladed turbine. (Guo et al., 2020) investigated the effect of the rear deflector on the Savonius turbine experimentally and numerically through towing tank experiments and 2D CFD simulations. The research shows that the power coefficient is less when the deflector length is shorter and the distance from the center of rotation is greater. The ideal position of the deflector is obtained by taking into account the engineering requirements of the power-producing unit. In this operating mode, the suppressing effect on the power coefficient is less than 3% when the distance from the center of rotation is 0.82 times the rotor's diameter. (Mereu et al., 2017) used the modeling method to investigate the interactions of several Savonius turbines in a linear array configuration with 2 to 16 turbines. The impact of key parameters such as distance between neighboring turbines and number of turbines is explored, and the linear array efficiency is determined. The collected findings suggest that as the space between the rotors decreases, performance improves, and efficiency increases for a larger number of turbines. Finally, there are a 19 percent increase in farm efficiency when the number of rotors was increased from two to sixteen. (Kerikous & Thévenin, 2019) planned to boost the output power by altering the blade profile of a hydraulic Savonius turbine. a Savonius turbine with varied blade forms on the concave and convex sides was designed using Computational Fluid Dynamics in order to increase the power coefficient  $C_p$ . Many transient computational fluid dynamics (CFD) simulations are carried out with the Star-CCM+ industrial flow simulation code, which is powered by the in-house optimization library OPAL++, which uses evolutionary techniques. At a tip speed ratio of 1.1, a higher mean of  $C_p$  of nearly 12% is achieved as compared to the typical Savonius turbine. Over the whole range of operation, the performance of the optimal shape was compared to that of the standard design. This comparison also demonstrated the efficacy has improved by over 15% at TSR of 1.2. (Setiawan et al., 2019) executed a round cylinder installation to improve the numerically simulated traditional savonius efficiency, to improve the positive torque, a cylinder was placed on the side of the advancing blade, and numerical study was performed without and with a circular cylinder. Using a 2D analysis of CFD simulation and moving mesh approach, a numerical analysis has been provided. Realizable k-epsilon (RKE) using second-order approach. The X/D parameter was changed from 0.0 to 2.0 with a 0.5 increase where D is the diameter of the blade and X is the horizontal distance between the axis of the

turbine and the cylinder. The highest findings of the numerical analysis revealed that the maximum power coefficient occurs at  $X/D = 0.5$ , and the best result of  $c_p$  is 0.250, with an increase of 17.31% at a TSR of 0.9. (Marmutova, 2016) confirmed and validated the Savonius published experimental data, using the 2D method of savonius turbine in Ansys Fluent® with the k-SST turbulence model. By improving the lift force, a suggested alteration of the rotor blade shape leads to a 2% gain in the power coefficient over a wide variety of tip speed ratios. The Ansys model was used to investigate Savonius' operation under unstable wind conditions. The Savonius' performance is affected by gustiness; it was discovered that with a greater level of gustiness, the rotor reaction is comparable to that of a rotor in a quasi-steady state. The wind characteristics: the probability density of wind speed or the probability density of wind power may affect the accuracy of the statistical procedure. (Zhou & Rempfer, 2013) aimed to build a simulation approach for forecasting the aerodynamic efficiency of a normal Savonius turbine and a Bach-type turbine by numerically exploring non-linear two-dimensional unsteady flow over a normal Savonius turbine and a Bach-type turbine. Star-CCM is used to do the simulations. A sliding mesh is used to solve the motion of the blades. The results of numerical simulations were compared to experimental results in a comparative examination of the two types of blades. The Bach-type turbine has been shown to have greater torque and power coefficient performance than the normal Savonius turbine. A full analysis of the respective flow field features, including the behavior of moment coefficients, velocity vectors, and pressure distribution, was offered to explain the causes of these variations. (Alom & Saha, 2019) studied the impact of blade profiles on rotor performance mathematically and experimentally. Modified Bach, Benesh, and elliptical shapes, as well as a traditional semi-circular shape, are used to simulate 2D unstable motion. With the assistance of a finite volume solution ANSYS Fluent, the simulation was carried out using the Shear Stress Transport k- $\omega$  turbulence model. At TSR = 0.8, the elliptical shape has a peak CP of 0.34, while the semicircular, Benesh, and modified Bach shapes have peak CPs of 0.272, 0.294, and 0.304, respectively. In comparison to the semicircular, the elliptical bladed rotor improves CP by 20.25 percent, while, Benesh and modified Bach turbines improved  $c_p$  by 19.49 percent, and 17.28 percent, respectively compared to the normal semicircular turbine. (Djanali et al., 2019) analyzed the Savonius turbine rotor is numerically using normal blades and Bach-profile blades with arc surface angles of 124 and 135. A half semi-circular rotor with an overlap was used as the conventional configuration. On the Savonius turbine, steady two-dimensional numerical simulations were done. The simulations were solved using the RANS solver with the turbulence method of the transition k- $\omega$  model. The calculations were carried out at constant velocities of 4 and 7 m/s, as well as at varied rotor angle locations. When compared it to a rotor with normal Savonius blades with overlap, the rotor with Bach-profile blades has a larger static torque coefficient. The Bach-profile blade has the best overall torque coefficient, with an arc surface of 135. The results obtained for very low velocities are similar to those found at greater velocities. (Pranta et al., 2021) studied the effect of modifying the rotor blade of the Savonius turbine to improve rotor performance.

Also looked at the principles of producing torque, the stream aspect, velocity, and pressure. The Finite Element Method is used to calculate energy and momentum equations. ANSYS-Fluent is used to create a 2-dimensional model for computational analysis for the savonius turbine. The Shear Stress Transport (SST) k- $\omega$  turbulence model was utilized to examine the behavior around the blade's specified geometries, and the proposed modified method was compared to a reference method based on an acceptable relationship with past investigations. The SST k- $\omega$  turbulence simulation The overall power output, power coefficients, and torque coefficients have increased reached to 18 percent, as a result of the refinement. (El-Askary et al., 2015) studied numerically the performance of the Savonius turbine with an overlap ratio of 0.15 with various changes in the design to increase rotor power. The authors applied the SST k- $\omega$  turbulence model based on past experiences. the new design captured incoming wind and form a wind jet on the advanced blade's concave side while keeping the return blade's convex surface out of the upwind stream. The fixed protective plates also stopped wind flow from reaching the convex surface of the return blades, preventing negative drag. Also, the results reveal that the new designs increase Savonius turbine performance in terms of power coefficient and torque coefficient. The results revealed that a suggested design with a curved passage shape has the greatest result, with wind speed having a substantial effect on it. However, noise generation was produced by wind flow vortex around and behind the suggested designs.

## 2. METHODOLOGY

### 2.1 Theoretical background:

The performance of the Savonius rotor can be stated in terms of coefficient of torque ( $C_m$ ) and coefficient of power ( $C_p$ ) and depend on the velocity of the wind and the tip speed ratio. TSR is the ratio of the tip blade speed to the wind speed across the blade.

The tip speed ratio (TSR) can be calculated using rotational velocity ( $w$ ) and free stream velocity ( $V$ ) measurements, defined as:

$$\lambda = \frac{V_{rotor}}{V} = \frac{\omega R}{V}$$

The moment coefficient can be determined using the dynamic torque recorded ( $T_d$ ) as follows:

$$C_m = \frac{4T_d}{\rho V^2 H D^2}$$

where  $H$  defined as the height of the rotor blade, and the coefficient of power is calculated as:

$$C_p = \frac{2T_d \omega}{\rho V^3 H D} = \lambda C_m$$

### 2.2 Geometry:

(Hayashi et al., 2005) had been designed the turbine's geometry, which may be shown in Fig.1. A typical blade is a traditional type of Savonius blade that consists of two semicircular blades. The turbine in Fig.1 has a diameter of  $D$ , a

is a shaft diameter that is in the center of a turbine, rotor diameter is  $L$ , and turbine overlap is  $O$ .

Table 1 shows the dimensions for the rotor in millimeters, where  $R$  is the radius of the rotor and  $A_s = D \cdot H$  is the swept area.

The simulation domain in this study has two basic zones: the inside domain and the outside domain. The rotating domain is the inside domain that closes to the rotor to represent the rotor mechanism. The diameter of the rotating domain is 1.36 times the size of the rotor. The outside domain is a fixed square, and the zone dimensions must be big enough to prevent any effect from the boundary conditions applied. the minimal size of the domain approved by (M. H. Mohamed et al., 2011) where the length is 20 times the turbine's radius. A length of  $24 \times R$  is used in this simulation as shown in Fig.2.

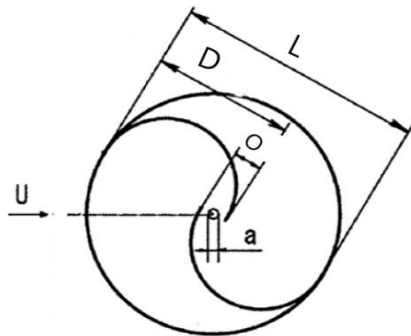


Figure 1. Geometry of savonius turbine by (Hayashi et al., 2005)

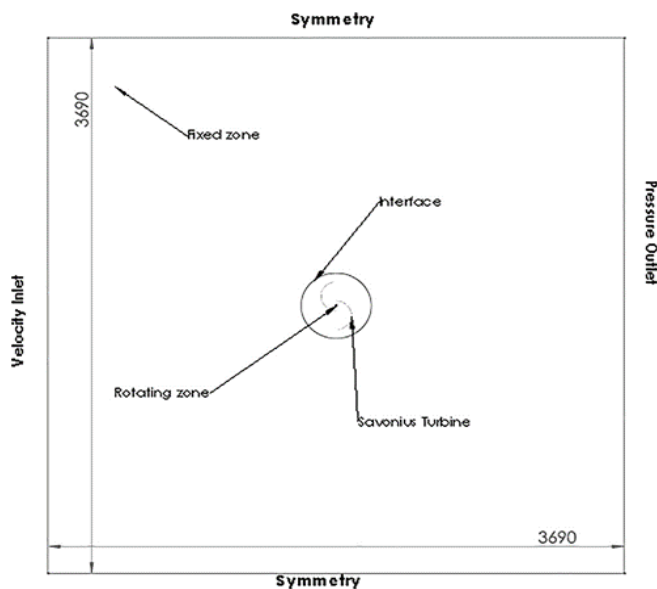


Figure 2. 2D computational domain for savonius turbine

### 2.3 Validation:

The accuracy and validity of the numerical model are validated using experimental data for (Hayashi et al., 2005) and numerical data for (Hassan Saeed et al., 2019) study. The two-dimensional calculation for two-bucket Savonius turbine

geometry was chosen and used to create and validate the numerical model. Figure 1 shows the chosen geometry, while Table 1 lists the turbine dimensions depending on (Hassan Saeed et al., 2019) study.

Table 1. The dimensions of the savonius turbine in mm

D	L	t	a/D	O/D	R	$D_0/L$
198	330	2	0.075	0.33	$D/2$	1.36

### 2.4 Mesh generation:

The mesh is one of the most significant simulation tools for achieving high accuracy and avoiding convergence problems. Because this model prevents mesh damage, the sliding mesh model (SSM) is employed to simulate the rotating turbine. Two domains were selected to employ this method: rotating domain and fixed domain. An unstructured triangular mesh is utilized for both fixed and rotating grids to reduce time while creating CFD simulations. The shape of the rotating domain is moving and circular and its mesh size has to be smaller enough to enhance the accuracy, the shape of the fixed domain is square and stationary, and its mesh size has to be bigger enough than the rotating domain to save time on the fluent program.

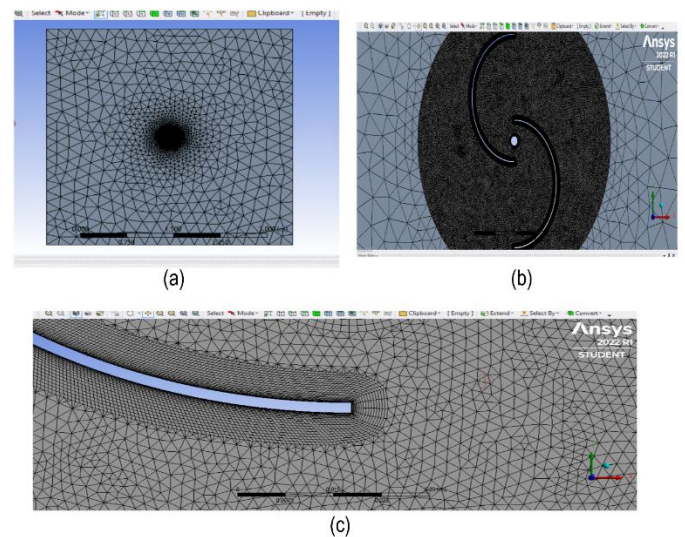


Figure 3 (a) The triangular meshing of savonius turbine. (b) Showed the triangular meshing of the rotating zone. (c) The inflation layers around the blade of savonius turbine.

As shown in fig.3 there are 20 layers of inflation surrounding the savonius blade with growth rates equal to 1.2. The interface boundary separates between rotating and fixed domains in Fig. 3(b), as well as the mesh size on both sides of the interfaces should be the same. For precise calculations, the revolving grids have a high smoothing factor. The number of mesh elements in the computational domain affects the moment and power coefficients where the power coefficient values were stable between 124,020 and 200,060 mesh elements as shown in fig 4. The total number chosen of mesh elements of conventional savonius turbine (without adding micro-cylinder

to turbine) was 124,020 elements. Taking that into account, with the inclusion of the micro-cylinder, the number of elements will slightly increase. The change in average Y plus

value in the last two models are negligible and the Y plus value is equal to one ( $Y^+=1$ ), as seen in figure 5.

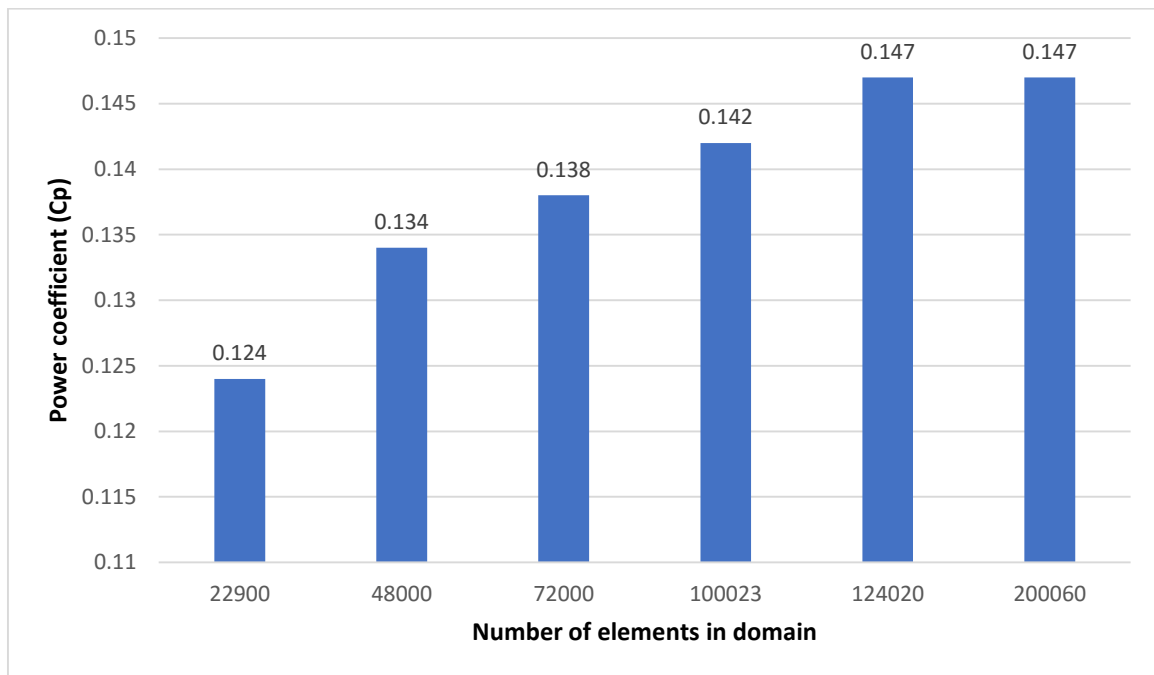


Figure 4. Variation of power coefficient with number of elements at  $\lambda=0.8$  for classical Savonius turbine

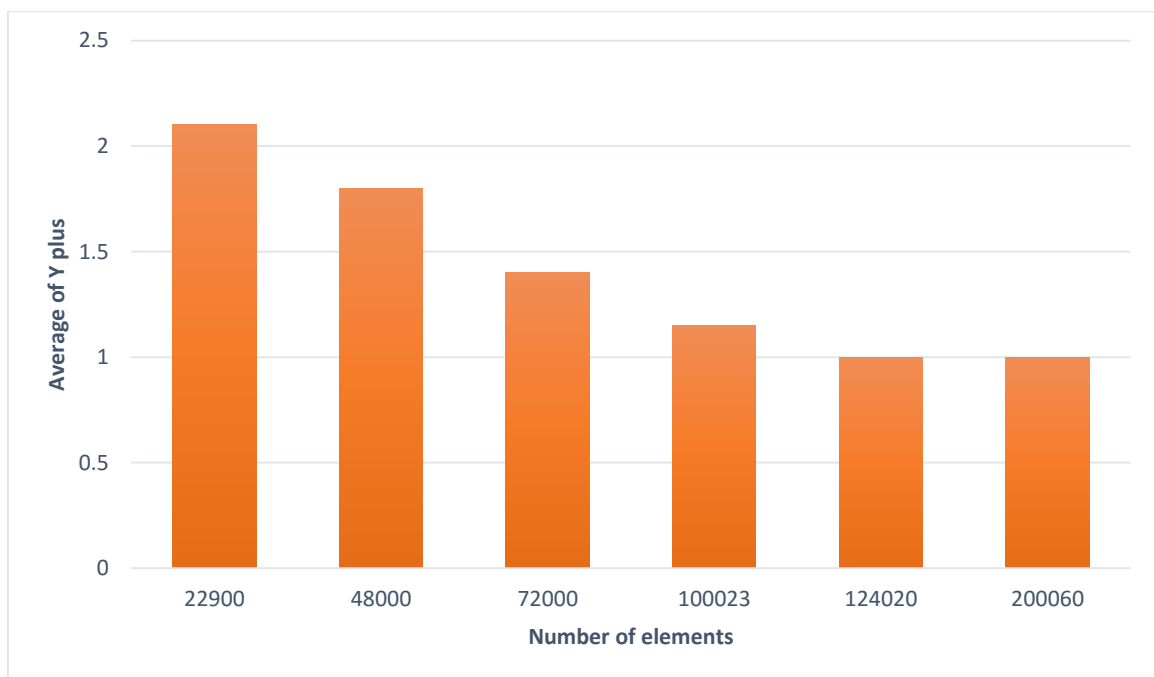


Figure 5. Variation of average Y plus with different number of elements at  $\lambda=0.8$  for classical Savonius turbine

## 2.5 Numerical solution and boundary conditions

Commercial ANSYS Fluent software based on the finite volume method was used for all simulations in this paper. The Unsteady Reynolds Average Navier-Stokes (URANS)

equations for unsteady-state incompressible flow are merged with the Shear Stress Transport ( $k-\omega$  SST) turbulence model for the current numerical analysis. The SIMPLE pressure-based solver is chosen for Computational Fluid Dynamics (CFD) simulations. Second-order calculations are utilized for

momentum equations, pressure calculations, and turbulent kinetic energy equations to get more high accurate results. The Shear Stress Transport (k- $\omega$  SST) turbulence model was tested with the variation of tip speed ratio TSR varying from 0.6 to 1 as shown in Table 2.

Table 2. Angular velocities( $\omega$ ) for tip speed ratio ( $\lambda$ )

TSR ( $\lambda$ )	0.6	0.7	0.8	0.9	1
$\omega$ (RPM)	313	365	417	469	521

The current work used two-dimensional (2D) simulations to improve the computational capacity. The fixed and rotating zones are the two major domains in this simulation. The velocity input and pressure output are in the fixed zone with a wind speed magnitude equal to 9 m/s. In the rotating zone, the blades rotate counterclockwise with a time steps calculating depend on the angular velocity as suggested by (Hassan Saeed et al., 2019). The main features of the validation model are summarized in table 3.

Table 3. The parameters of tested model

Parameters	Description
Wind speed inlet (U)	9 m/s
Tip speed ratio $\lambda$	0.6-1
Fluid	Air
Turbulence model	K- $\omega$ (SST)
Residual	$1 \times 10^{-5}$
Pressure outlet	Atmospheric pressure
Side	Symmetry

### 2.6 Result of the validation:

Verification is required for any numerical project. It is critical to examine and validate the data on the first flight to ensure accuracy. If the data is correct, the results will be correct as well. The current model is shown to be compatible with (Hassan Saeed et al., 2019) model. The current CFD model's power coefficient is roughly comparable to Hassan's. The comparison in figure 6 shows that the current model's outcomes are acceptable.

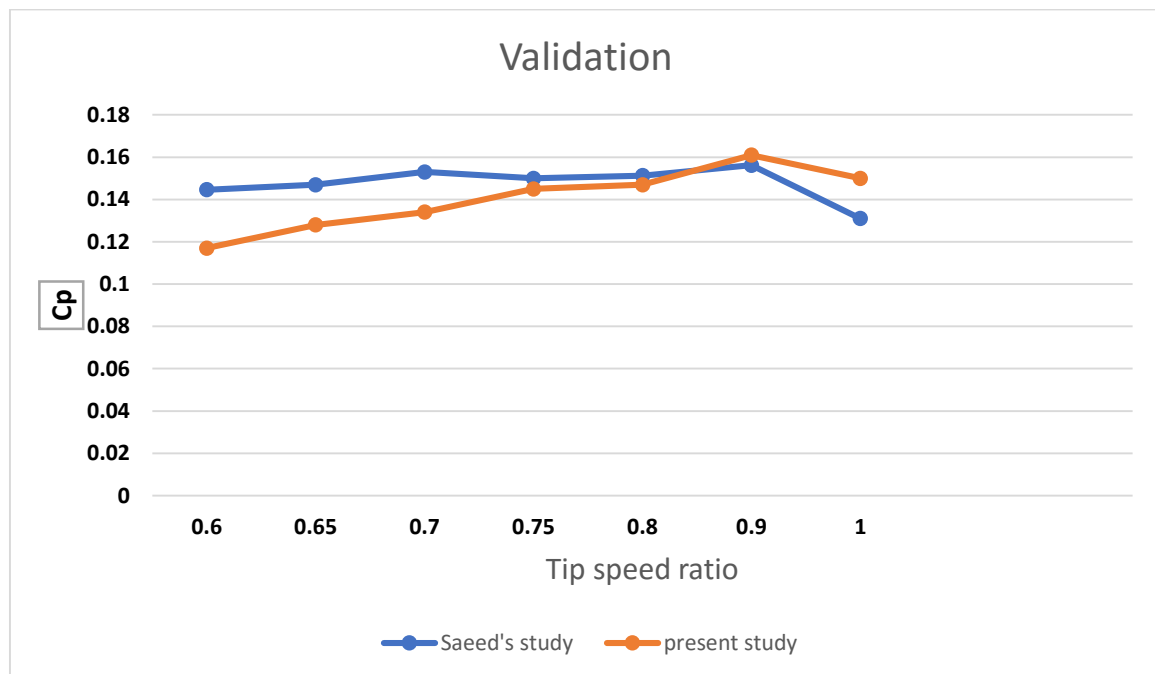


Figure 6 Validation curve of power coefficient with numerical results of (Hassan Saeed et al., 2019)

## 3. RESULTS AND DISCUSSION

### 3.1 Geometry of the cylinder:

A micro circular cylinder installed on the upstream side of the returned blade causes the formation of a wake region between the micro cylinder and the returned blade; this area has a pressure drop. Moreover, the micro cylinder will passively

regulate the flow around the returned blade and affect the pressure distribution on the returned rotor blade. As a result, the change in pressure between the front and back sides of the returned blade diminishes, lowering the pressure drag of the returned blade. As a result, the drag force of the returned blade decreases, resulting in a positive torque in the rotor.

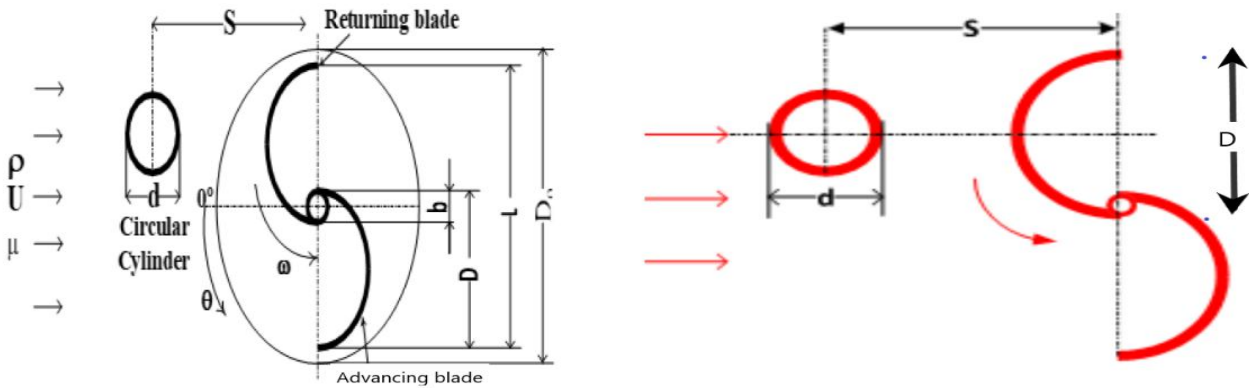


Figure 7. Geometry design of a savonius turbine with a circular cylinder installed on the upstream side of the returned blade.

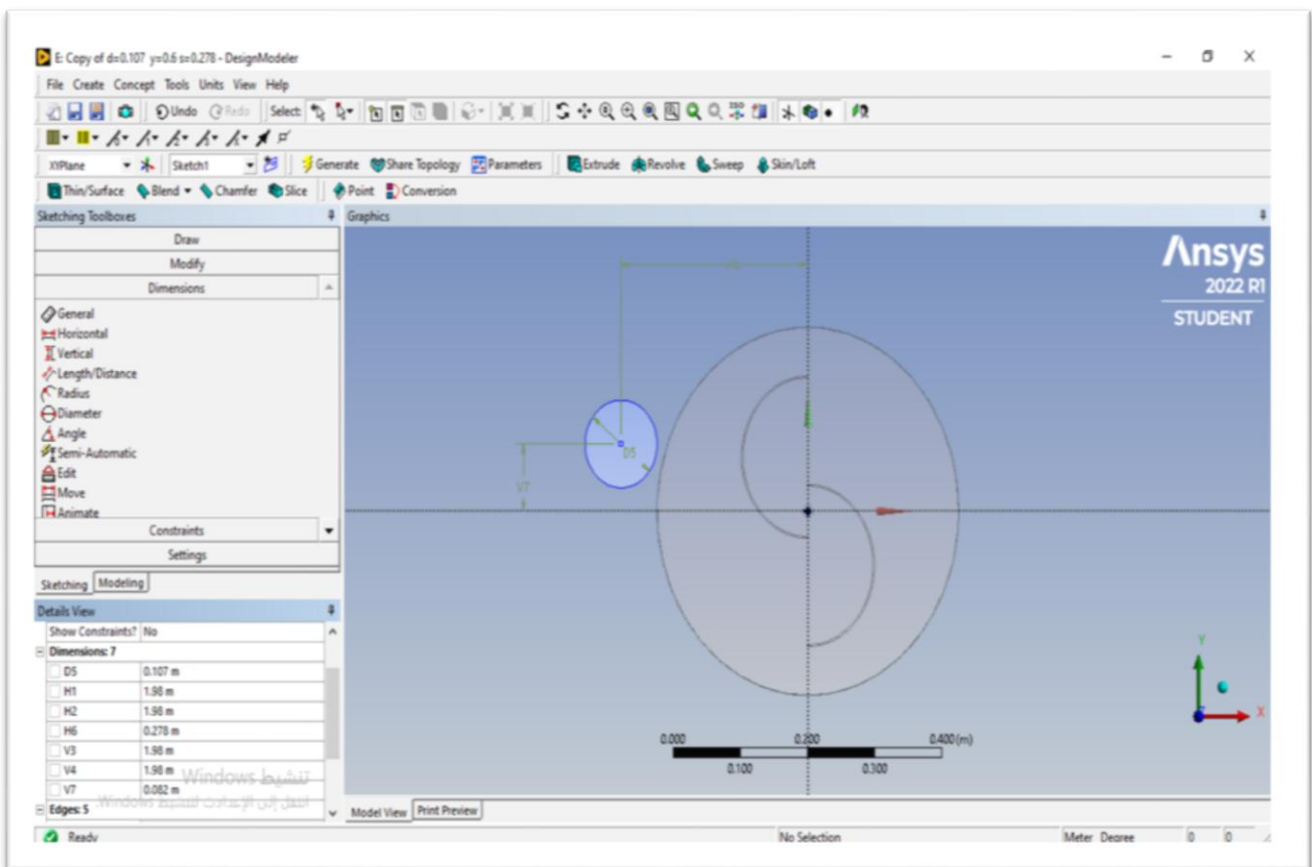


Figure 8. Savonius turbine with a circular cylinder installed on the upstream side of the returned blade.

The results discuss the impact of adding a micro-cylinder to savonius wind turbine (classical turbine). There are three states of adding a micro-cylinder to a savonius turbine (classical turbine) based on the diameter of the cylinder and the distance between the blade and the cylinder and the height of the cylinder.

- 1- The first section will discuss the effects of increasing the cylinder diameter ( $d/D=0.45, 0.54, 0.60$ ) at the same location and the same distance between the cylinder and the blade ( $S/D=1.4$ ).
- 2- The second section will discuss the effects of increasing the distance between the blade and the cylinder ( $S/D=1.4, 1.6, 1.8$ ) with the same cylinder diameter and the same height of the cylinder ( $d/D=0.54, h/R=0.50$ ).
- 3- The third section investigates the effects of changing the height of the micro-cylinder vertical axis around the blade ( $h/R=0.40, 0.50, 0.60$ ) at the same distance between the blade and the cylinder and the same cylinder diameter ( $d/D=0.54, S/D=1.4$ ).



There are seven cases of the cylinder that are studied depending on the cylinder diameter and horizontal distance and vertical distance for the cylinder and then drawing a curve power

coefficient and torque coefficient for each case. Table 4 shows the properties of each case.

Table 3 RC Properties at various diameters and locations of the cylinder adding to the savonius turbine

Case Name	Case Properties		
	d/D	S/D	The height /the radius of the rotor (h/R)
RC 1	0.45	1.4	0.50
RC 2	0.54	1.4	0.50
RC 3	0.60	1.4	0.50
RC 4	0.54	1.6	0.50
RC 5	0.54	1.8	0.50
RC 6	0.54	1.4	0.40
RC 7	0.54	1.4	0.60

## 2.2 The impact of change in cylinder diameters (d)

The effect of adjusting the diameter of the cylinder is studied in this section. The cylinder diameter per blade diameter ratios (0.45, 0.54, and 0.60) are investigated at the same speed (U) of 9 m/s while the cylinder is kept at the same distance  $S/D = 1.4$  and the same height ( $h/R = 0.50$ ). compares the power

coefficient ( $C_p$ ) and torque coefficient ( $C_m$ ) for multi-diameter cylinders adding to classical Savonius turbine with different tip speed ratios ( $k$ ). as shown in fig. 9 and fig. 10 the three different diameters have a positive impact on the power generated compared with the classical turbine. Particularly, the case RC2 ( $d/D=0.54$ ) showed better performance when compared to the other two diameters.

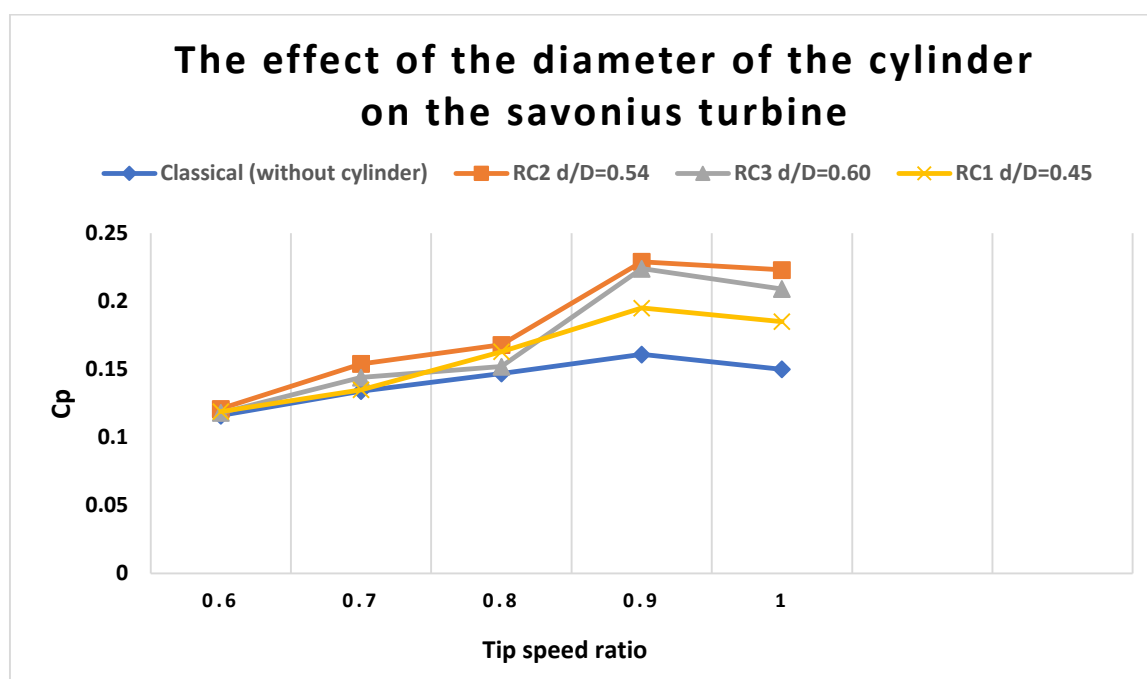


Figure 9 The impact of change in cylinder diameters on the power coefficient per tip speed ratio.

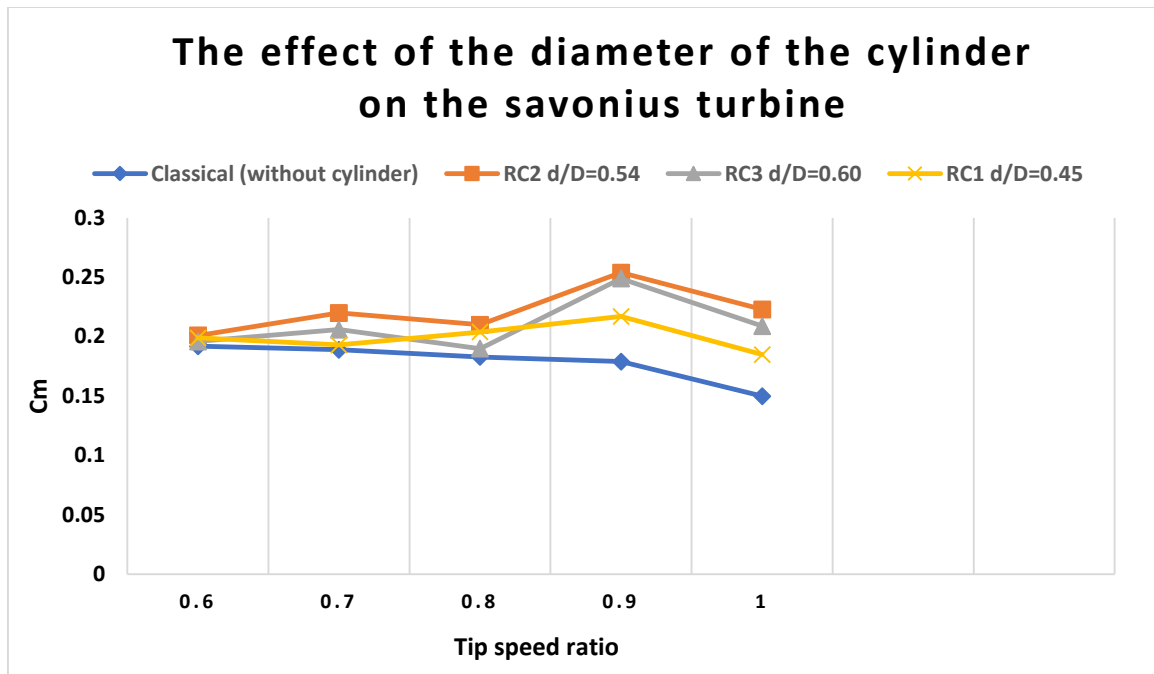


Figure 10 The impact of change in cylinder diameters on the torque coefficient per tip speed ratio

### 2.3 Effect of change in the horizontal distance (S):

The impact of adjusting the horizontal distance of the cylinder relative to the returning blade is studied in this section. The horizontal distance (S) per blade diameter (D) ratios (1.4, 1.6, and 1.8) (RC2, RC4, RC5) are investigated at the same speed (U) of 9 m/s while the cylinder is kept at the same diameter  $d/D = 0.54$  and the same height ( $h/R = 0.50$ ). compares the

coefficient of power ( $C_p$ ) and torque coefficient for multi-distance of the cylinder adding to classical Savonius turbine with different tip speed ratios ( $k$ ). as shown in figure 11 the three different distances have a positive and negative impact on the power generated compared with the classical turbine. Particularly, the case RC2 ( $S/D=1.4$ ) showed better performance when compared to the other two cases.

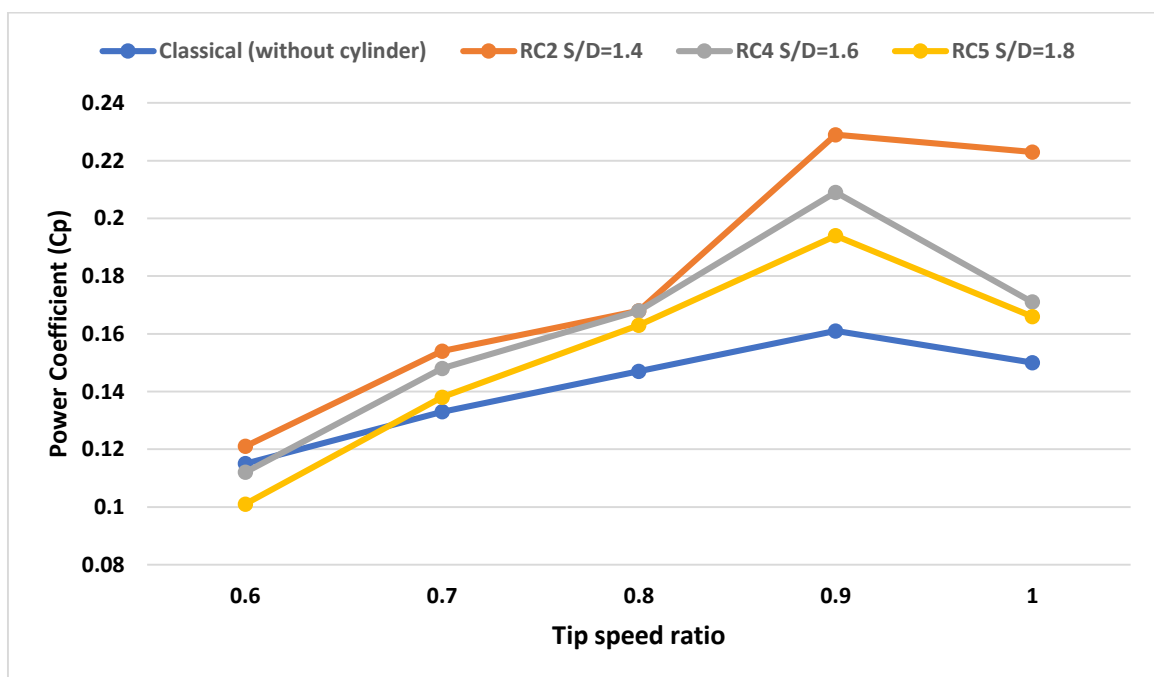


Figure 11 Effect of change in the horizontal distance (S) on the power coefficient per tip speed ratio.

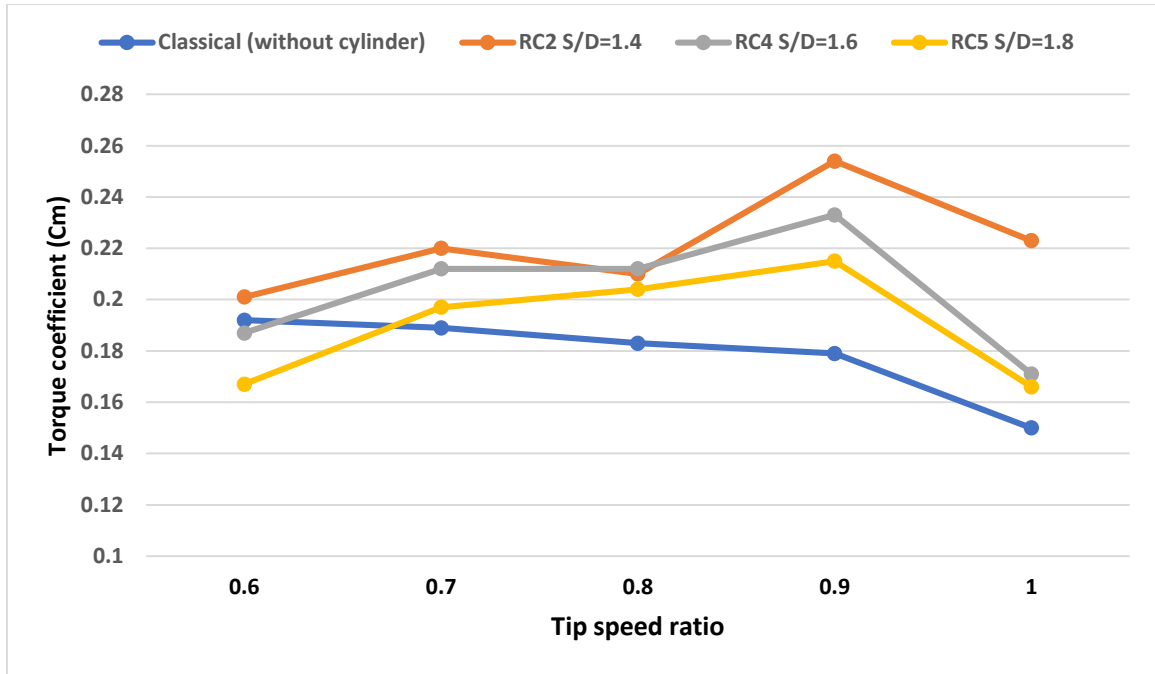


Figure 12 Effect of change in the horizontal distance (S) on the torque coefficient per tip speed ratio.

**2.4 Effect of change in the vertical height of the cylinder (h):**

In this part, the micro-cylinder is moved in a vertical axis close to the blade at the fixed diameter where, cylinder diameter per blade diameter ( $d/D=0.54$ ) that chose of the previous part, the effect of the micro-cylinder position in a vertical axis will be investigated in this section. The location change by vertical variable as shown in table 5. Three heights for the round cylinder are studied. Figure 13 and figure 14 display the power coefficient ( $C_p$ ) and torque coefficient ( $C_m$ ) relative to tip

speed ratio ( $\lambda$ ) at three different heights for adding round-cylinder (RC2, RC6, RC7) at the same speed (U) of 9 m/s while the cylinder is kept at the same horizontal distance  $S/D = 1.4$ . The relationship between tip speed ratio ( $\lambda$ ) and power coefficient ( $C_p$ ) shows in figure 13. The three different heights have a positive and negative impact on the power generated compared with the conventional turbine. Particularly, the case RC2 ( $h/R=0.50$ ) showed better performance when compared to the other two heights.

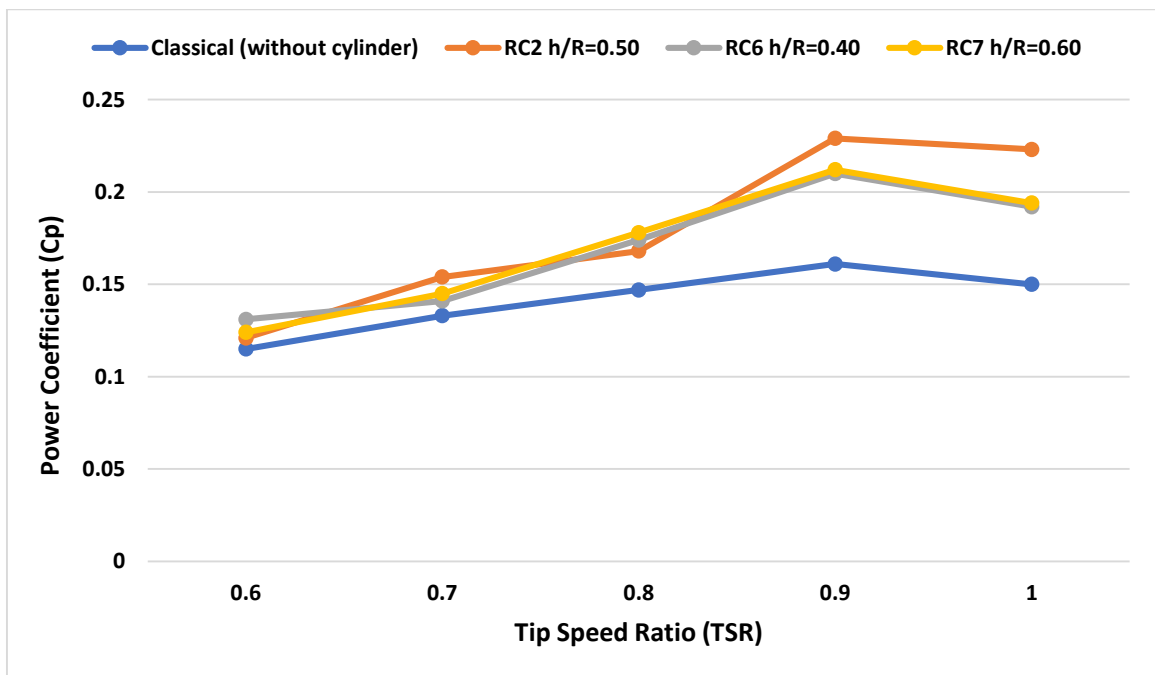


Figure 13 Effect of change in the vertical height (h) on the power coefficient per tip speed ratio

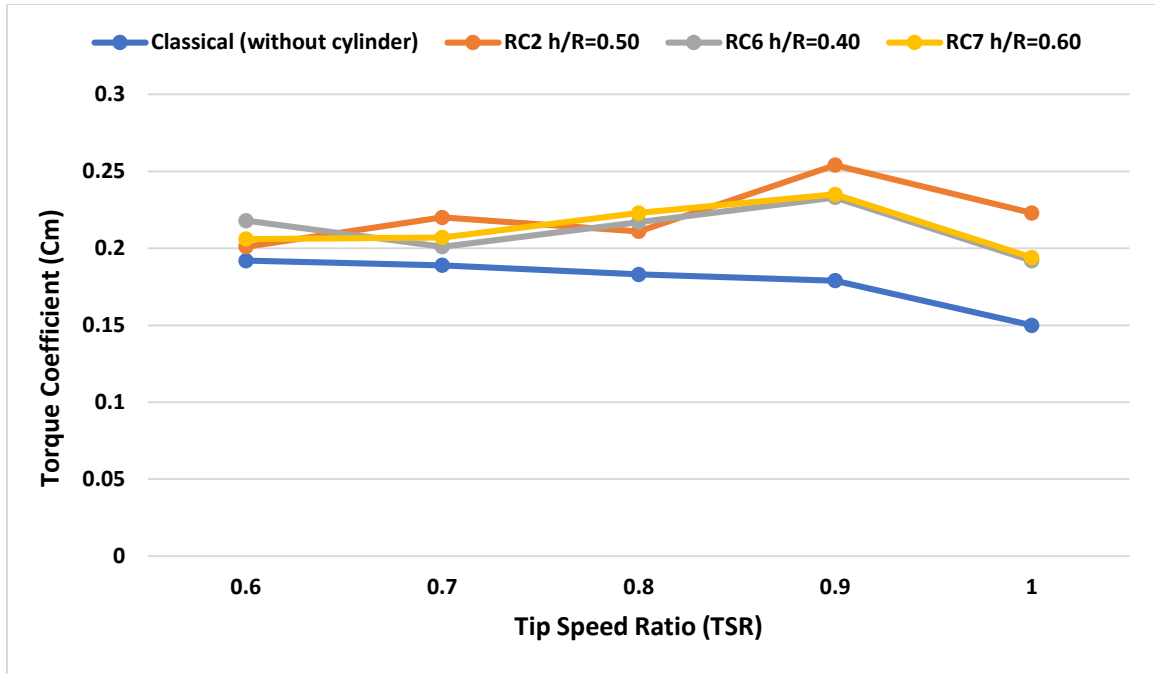


Figure 14 Effect of change in the vertical height (h) on the torque coefficient per tip speed ratio

As shown in the previous comparison figures, we get better performance at the location (RC 2), this location of the cylinder gives a better value for the power coefficients, especially at the tip speed ratio of 0.9 gives the best value of power coefficient

(Cp) equal 0.229 with increment by 42% in the performance of the savonius wind turbine. Figure 15 shows the comparison between the conventional turbine and the best case (RC2) of cylinder location relative to the power coefficient.

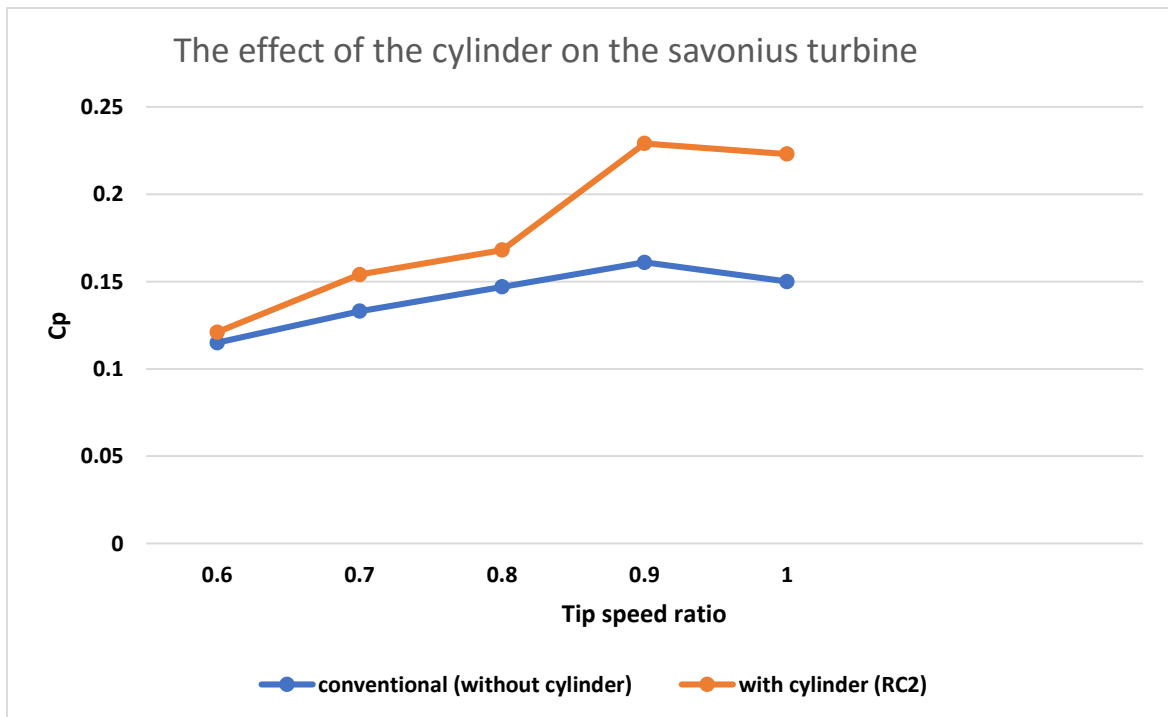


Figure 15 Effect of adding the cylinder on the power coefficient per tip speed ratio

Table 4 The percentage of increase in performance due to the addition of the cylinder per tip speed ratio

Tip speed ratio	C <sub>p</sub> for conventional turbine	C <sub>p</sub> for turbine with cylinder	(Relative Increment %) *
0.6	0.115	0.121	5.2
0.7	0.133	0.154	15.7
0.8	0.147	0.168	14.3
0.9	0.161	0.229	42.2
1	0.150	0.223	48.6

\* Relative Increment (%) = ((C<sub>p</sub> after adding the cylinder - C<sub>p</sub> for conventional turbine) / C<sub>p</sub> for conventional turbine) × 100

Table 5 shows the percentage of changes in the power coefficient due to adding the round cylinder to the turbine, in case (RC2) compared to the conventional turbine (without adding a cylinder to the turbine). The average power coefficient (C<sub>p</sub>) increases by (5.2 %, 15.7%, 14.3%, 42.2% and 48.6 %) for TSRs (0.6, 0.7, 0.8, 0.9 and 1) respectively. The best increment is at TSR=1 where the power coefficient (C<sub>p</sub>) increases by 46.6%. From among the five tip speed ratios proposed, the TSR equal to 0.9 is the highest performance, whereas the TSR equal to 0.6 is the lowest performance.

## CONCLUSIONS

The goal of this study is to investigate the ways to enhance the performance of the Savonius wind turbine numerically. It is accomplished by placing a round cylinder upstream of the Savonius wind rotor as a passive control. As a result, the drag force of the returned blade decreases, resulting in a positive torque in the rotor and improving the performance of the Savonius turbine. The influence of the cylinder on the Savonius turbine has been numerically studied by 2D CFD simulations using Inventor software to draw a 2D model of the turbine. The analyses were carried out utilizing the ANSYS Fluent and the Shear Stress Transport k- $\omega$  turbulence model. Seven cases are studied with different diameters and locations of the micro-cylinder. The following is a summary of the research results:

- The three different diameters have a positive impact on the power generated compared with the classical turbine. Particularly, the case RC2 (d/D=0.54) showed better performance when compared to the other two diameters.
- The three different distances have a positive and negative impact on the power generated compared with the classical turbine. Particularly, the case RC2 (S/D=1.4) introduced better performance when compared to the other two cases.
- The three different heights have a positive and negative impact on the power generated compared with the conventional turbine. Particularly, the case RC2 (h/R=0.50) revealed best performance when compared to the other two heights.

- The location (RC2) of the cylinder gives a better value for the power coefficients, especially at the tip speed ratio of 0.9 which gives the best value of power coefficient (C<sub>p</sub>) equal 0.229 with increment by 42% in the performance of the savonius wind turbine.
- The best increment is at TSR=1 where the power coefficient (C<sub>p</sub>) increases by 46.6%. From among the five tip speed ratios proposed, the TSR equal to 0.9 is the highest performance, whereas the TSR equal to 0.6 is the lowest performance.

## REFERENCES

- Alharbi, F., & Csala, D. (2020). Saudi Arabia's solar and wind energy penetration: Future performance and requirements. *Energies*, 13(3). <https://doi.org/10.3390/en13030588>
- Alizadeh, H., Jahangir, M. H., & Ghasempour, R. (2020). CFD-based improvement of Savonius type hydrokinetic turbine using optimized barrier at the low-speed flows. *Ocean Engineering*, 202(August 2019), 107178. <https://doi.org/10.1016/j.oceaneng.2020.107178>
- Alom, N., Kumar, N., & Saha, U. K. (2017). Aerodynamic performance of an elliptical-bladed savonius rotor under the influence of number of blades and shaft. *ASME 2017 Gas Turbine India Conference, GTINDIA 2017*, 2, 1–11. <https://doi.org/10.1115/GTINDIA2017-4954>
- Alom, N., & Saha, U. K. (2019). Influence of blade profiles on Savonius rotor performance: Numerical simulation and experimental validation. *Energy Conversion and Management*, 186(October 2018), 267–277. <https://doi.org/10.1016/j.enconman.2019.02.058>
- Barhouni, E. M., Okonkwo, P. C., Zghaibeh, M., Belgacem, I. Ben, Alkanhal, T. A., Abo-Khalil, A. G., & Tlili, I. (2020). Renewable energy resources and workforce case study Saudi Arabia: review and recommendations. *Journal of Thermal Analysis and Calorimetry*, 141(1), 221–230. <https://doi.org/10.1007/s10973-019-09189-2>
- Bouzaher, M. T. (2022). Effect of flexible blades on the Savonius wind turbine performance. *Journal of the Brazilian Society of Mechanical Sciences and Engineering*, 44(2), 1–16. <https://doi.org/10.1007/s40430-022-03374-5>
- Djanali, V. S., Fathurrahman, Z., Dwiyanoro, B. A., & Ikhwan, N. (2019). Numerical study of savonius wind turbines with

- standard and Bach-profile blade variations. *AIP Conference Proceedings*, 2187(December).  
<https://doi.org/10.1063/1.5138296>
- Ebrahimpour, M., Shafaghat, R., Alamian, R., & Shadloo, M. S. (2019). Numerical investigation of the Savonius vertical axis wind turbine and evaluation of the effect of the overlap parameter in both horizontal and vertical directions on its performance. *Symmetry*, 11(6).  
<https://doi.org/10.3390/sym11060821>
- El-Askary, W. A., Nasef, M. H., AbdEL-hamid, A. A., & Gad, H. E. (2015). Harvesting wind energy for improving performance of savonius rotor. *Journal of Wind Engineering and Industrial Aerodynamics*, 139, 8–15.  
<https://doi.org/10.1016/j.jweia.2015.01.003>
- Guo, F., Song, B., Mao, Z., & Tian, W. (2020). Experimental and numerical validation of the influence on Savonius turbine caused by rear deflector. *Energy*, 196.  
<https://doi.org/10.1016/j.energy.2020.117132>
- Hadi Ali, M. (2013). Experimental Comparison Study for Savonius Wind Turbine of Two & Three Blades At Low Wind Speed. *International Journal of Modern Engineering Research (IJMER) Www.Ijmer.Com*, 3(5), 2978–2986.
- Hassan Saeed, H. A., Nagib Elmekawy, A. M., & Kassab, S. Z. (2019). Numerical study of improving Savonius turbine power coefficient by various blade shapes. *Alexandria Engineering Journal*, 58(2), 429–441.  
<https://doi.org/10.1016/j.aej.2019.03.005>
- Hayashi, T., Li, Y., & Hara, Y. (2005). Wind tunnel tests on a different phase three-stage Savonius rotor. *JSME International Journal, Series B: Fluids and Thermal Engineering*, 48(1), 9–16.  
<https://doi.org/10.1299/jsmeb.48.9>
- Kacprzak, K., & Sobczak, K. (2015). *Computational assessment of the influence of the overlap ratio on the power characteristics of a Classical Savonius wind turbine*. 314–322. <https://doi.org/10.1515/eng-2015-0039>
- Kerikous, E., & Thévenin, D. (2019). Optimal shape of thick blades for a hydraulic Savonius turbine. *Renewable Energy*, 134(August 2019), 629–638.  
<https://doi.org/10.1016/j.renene.2018.11.037>
- Mao, Z., & Tian, W. (2015). Effect of the blade arc angle on the performance of a Savonius wind turbine. *Advances in Mechanical Engineering*, 7(5), 1–10.  
<https://doi.org/10.1177/1687814015584247>
- Marmutova, S. (2016). Performance of a Savonius wind turbine in urban sites using CFD analysis. In *University of Vaasa*.
- Mereu, R., Federici, D., Ferrari, G., Schito, P., & Inzoli, F. (2017). Parametric numerical study of Savonius wind turbine interaction in a linear array. *Renewable Energy*, 113, 1320–1332. <https://doi.org/10.1016/j.renene.2017.06.094>
- Mohamed, M. H., Janiga, G., Pap, E., & Thévenin, D. (2011). Optimal blade shape of a modified Savonius turbine using an obstacle shielding the returning blade. *Energy Conversion and Management*, 52(1), 236–242.  
<https://doi.org/10.1016/J.ENCONMAN.2010.06.070>
- Mohamed, Mohamed H., Alqurashi, F., & Thévenin, D. (2021). Performance enhancement of a Savonius turbine under effect of frontal guiding plates. *Energy Reports*, 7, 6069–6076. <https://doi.org/10.1016/J.EGYR.2021.09.021>
- Pranta, M. H., Rabbi, M. S., & Roshid, M. M. (2021). A computational study on the aerodynamic performance of modified savonius wind turbine. *Results in Engineering*, 10(February), 100237.  
<https://doi.org/10.1016/j.rineng.2021.100237>
- Roy, S., Das, R., & Saha, U. K. (2018). An inverse method for optimization of geometric parameters of a Savonius-style wind turbine. *Energy Conversion and Management*, 155(October 2017), 116–127.  
<https://doi.org/10.1016/j.enconman.2017.10.088>
- Said, S. A. M., El-Amin, I. M., & Al-Shehri, A. M. (2004). Renewable Energy Potentials in Saudi Arabia. *Beirut Regional Collaboration Workshop on Energy Efficiency and Renewable Energy Technology, American University of Beirut, October*, 76–82.
- Sakti, G., & Yuwono, T. (2021). NUMERICAL AND EXPERIMENTAL INVESTIGATION OF THE EFFECT OF A CIRCULAR CYLINDER AS PASSIVE CONTROL ON THE SAVONIUS WIND TURBINE PERFORMANCE. *Journal of Southwest Jiaotong University*, 56(6), 73–93.  
<https://doi.org/10.35741/issn.0258-2724.56.6.7>
- Sanusi, A., Soeparman, S., Wahyudi, S., & Yuliati, L. (2016). *Experimental Study of Combined Blade Savonius Wind Turbine. September 2017*.
- Setiawan, P. A., Yuwono, T., Widodo, W. A., Julianto, E., & Santoso, M. (2019). Numerical study of a circular cylinder effect on the vertical axis savonius water turbine performance at the side of the advancing blade with horizontal distance variations. *International Journal of Renewable Energy Research*, 9(2), 978–985.  
<https://doi.org/10.20508/ijrer.v9i2.8890.g7662>
- Shaheen, M., El-Sayed, M., & Abdallah, S. (2015). Numerical study of two-bucket Savonius wind turbine cluster. *Journal of Wind Engineering and Industrial Aerodynamics*, 137, 78–89. <https://doi.org/10.1016/j.jweia.2014.12.002>
- Sobczak, K., Obidowski, D., Reorowicz, P., & Marchewka, E. (2020). Numerical investigations of the savonius turbine with deformable blades. *Energies*, 13(14).  
<https://doi.org/10.3390/en13143717>
- Submitted, T. (2017). *Aerodynamic Shape Optimization of Savonius Wind Turbines. July*.
- Talukdar, P. K., Sardar, A., Kulkarni, V., & Saha, U. K. (2018). Parametric analysis of model Savonius hydrokinetic turbines through experimental and computational investigations. *Energy Conversion and Management*, 158(October 2017), 36–49.  
<https://doi.org/10.1016/j.enconman.2017.12.011>
- Zhou, T., & Rempfer, D. (2013). Numerical study of detailed flow field and performance of Savonius wind turbines. *Renewable Energy*, 51(March 2013), 373–381.  
<https://doi.org/10.1016/j.renene.2012.09.046>